

Size and resin fractionations of dissolved organic matter and characteristics of disinfection by-product precursors in a pilot-scale constructed wetland

Jiachang Pi, Guangcan Zhu, Lianqing Liu, Chuya Wang and Zhonglian Yang

ABSTRACT

Controlling the formation of disinfection by-products (DBPs) is a major issue in the drinking water industry, and understanding the characteristics of DBP precursors in treatment processes for micro-polluted raw water is key to improving water quality. In this study, a sampling program was undertaken to investigate the fate of dissolved organic matter (DOM) and the characteristics of DBP precursors in a pilot constructed wetland imitating the Yanlong Lake ecological project. Using XAD resin adsorption and ultrafiltration techniques, the dissolved organic carbon, UV_{254} , and DBP formation potential (DBPFP) were measured in different DOM fractions in raw water and wetland effluents. After the constructed wetland treatment, the low molecular weight fraction (<3 kDa) of DOM and DBPFP generally showed a decreasing trend along the water path, while the high molecular weight fraction (>3 kDa) of DOM increased. The specific DBPFP (SDBPFP) was much higher in the <1 kDa fraction than in the other fractions. Although the hydrophobic fraction of DOM was the most abundant in all stages of the wetland treatment, the SDBPFP of the hydrophilic fraction was higher than that of the hydrophobic fraction. Furthermore, compared with raw water, the DOC, UV_{254} and DBPFP in the treated wetland effluents increased; however, all of the chemical DOM fractions exhibited decreased SDBPFP in accordance with a decrease in the specific ultraviolet absorbance during wetland treatment. These conclusions indicate that the DOM produced by the wetland system may generate DBPs less readily compared with the DOM of raw water.

Key words | disinfection by-product precursors, dissolved organic matter (DOM), hydrophobic/hydrophilic, micro-polluted raw water, molecular weight

HIGHLIGHTS

- The constructed wetland system of water source area would reduce small molecular weight DOM but increase large molecular weight DOM.
- The chemical fraction of SUVA and SDBPFP decreased along the wetlands treatment path.
- DOM produced by the wetland system may generate DBPs less readily compared with the DOM of raw water.

INTRODUCTION

In China, due to rapid development of industry and agriculture, approximately 60% of urban drinking water sources

are polluted to varying degrees (Wang & Wang 2000). To ensure the safety and quality of drinking water and respond to sudden pollution incidents, construction of storage reservoirs incorporating artificial wetlands and other ecological mitigation measures has become an economically favorable alternative to energy-intensive engineered treatment plant

This is an Open Access article distributed under the terms of the Creative Commons Attribution Licence (CC BY 4.0), which permits copying, adaptation and redistribution, provided the original work is properly cited (<http://creativecommons.org/licenses/by/4.0/>).

doi: 10.2166/ws.2021.013

Jiachang Pi
Guangcan Zhu (corresponding author)
Lianqing Liu
Chuya Wang
Zhonglian Yang
School of Energy and Environment, Southeast University,
Nanjing 210096,
People's Republic of China
and
State Key Laboratory of Environmental Medicine Engineering, Ministry of Education, Southeast University,
Nanjing 210096,
People's Republic of China
E-mail: gc-zhu@seu.edu.cn

approaches to improving the quality of raw water (Haynes 2015). Chenhang Reservoir and Jinze Reservoir in Shanghai and the Shiyaoyang Water Source Ecological Wetland Project in Jiaxing City are examples of such ecological storage reservoirs, which provide water storage capacity and improve raw water quality by artificially strengthening the purification function of the ecosystem (Huang 2000; Dierberg *et al.* 2002; Iamchaturapatr *et al.* 2007; Schipper & McGill 2008). Constructed wetlands lower inorganic nutrient inputs but enhance dissolved organic matter (DOM) loadings into drinking water reservoirs, due to the metabolic effects of aquatic organisms (Scholz *et al.* 2016; Hansen *et al.* 2018). Most water supply plants in China require chlorine disinfection, and the DOM can form disinfection by-products (DBPs) such as trihalomethanes (THMs) and haloacetic acids (HAAs), the two most prevalent classes among hundreds of DBPs regulated by the U.S. (McGeekin *et al.* 1995; Rostad *et al.* 2000). A large body of research has demonstrated that exposure to DBPs can increase the risk of cancer and reproductive disorders (Richardson *et al.* 2007); therefore, research on the causes and mechanisms of DBP formation in reservoirs has become an important focus in the last two decades.

Plant root and microorganism exudates play an important role in the DOM composition of wetland systems. They contain many components including sugars and polysaccharides, organic and amino acids, peptides, and proteins (Hinsinger *et al.* 2006), and plant and microorganism metabolism can induce a significant shift in the composition of DOM. For example, an influent of relatively unstable alcohols and olefins was converted to stable aromatics and alkyl hydrocarbons in the effluent (Li *et al.* 2008). However, aromatic substances contribute more to the formation of carbonaceous and nitrogenous DBPs (Zhou *et al.* 2015), and the studies by Hua & Reckhow (2007) and Zhi-sheng *et al.* (2009) also demonstrated that aromatic compounds react easily with chlorine to form DBPs such as THMs and HAAs. Yang *et al.* (2016) used a vertical subsurface flow constructed wetland and surface wetland tandem system to treat micro-polluted raw water in the Yangtze River and found that the THM formation potential (THMFP) of the system effluent increased by 20.52% compared with the influent water. DOM in the roots and leaves of plants also has an effect on DBP production, and soluble microbial products and aromatic

proteinaceous substances (polyphenols) can enhance the THMFP (Wei *et al.* 2009). In addition, aquatic animals often breed prolifically in ecological engineering sites, and the amino acids, proteins, and fats contained in their metabolites can also act as precursors for DBPs (Sun *et al.* 2014). However, although previous studies have indicated that the DOM produced by plants and animals in wetlands may act as precursors for DBPs, field investigations and characterization of DOM in constructed wetlands have received only limited research attention.

DOM from wetlands is a heterogeneous mixture of complex organic materials including humic substances, hydrophilic acids, proteins, lipids, carboxylic acids, polysaccharides, amino acids, and hydrocarbons (Leenheer & Croué 2003; Cheng *et al.* 2005). It is impossible to identify and investigate these compounds individually; therefore, the preferred method for evaluating DBP precursors is classification of DOM in water bodies based on a given characteristic and measurement of the reaction behavior of the DOM with this characteristic. Resin adsorption (RA) and ultrafiltration have been widely and successfully applied in characterizing the chemical and physical properties of DOM from natural waters (Wei *et al.* 2008). In particular, the XAD-8 and XAD-4 resins have been widely used to separate DOM into hydrophobic (HPO) and hydrophilic (HPI) components (Leenheer 1981).

The purpose of this work is to evaluate the behaviors and characteristics of DBP precursors in three types of wetlands that form an ecological engineering system for a water source with micro-polluted raw water, by analyzing the molecular weight distribution and chemical fractionation of DOM. Dissolved organic carbon (DOC) and UV₂₅₄ values were measured to investigate the variation patterns of different molecular weight and chemical fractions. Additional experiments were conducted to evaluate the DBP formation potential (DBPFP) of each weight and chemical fraction in raw water and wetland effluent.

MATERIALS AND METHODS

Constructed wetlands

Experiments were carried out in three different types of constructed wetlands: a surface wetland, submerged plant pond,

and ecological pond, hereafter named wetland A, B, and C. The constructed wetlands (Figure 1) were located within a pilot plant on one of the inflow streams of a drinking water reservoir in Yancheng City, Jiangsu Province, China, designed to imitate the Yanlong Lake ecological project (a replicated field-scale study). In this pilot plant, raw water from the Viper River is driven into a high water tank by a lifting pump and then passed through wetland A, B, and C successively under gravity. A schematic diagram of the composite constructed wetland is presented in Figure 1.

The water quality parameters of raw water from the Viper River, collected from March 2017 to February 2018 (the most recent available year), are summarized in Table 1. The wetlands were planted with emergent and submerged plants in June 2017; seedlings of the plants listed in Table 2 were transplanted from a local natural field to the wetlands. In addition, a non-classical biological manipulation technique was adopted in wetland C: silver carp and bighead carp were added to control the algae density in the raw water and prevent eruption of cyanobacteria, which are detrimental to water quality. The total density of carp was 30 g m^{-3} , and the quantity ratio of silver carp to bighead carp was 2:1. Some of the wetland parameters and installation compositions are listed in Table 2. After planting and enriching with fish, the influent flow was gradually increased from 0.3 to $0.6 \text{ m}^3 \text{ days}^{-1}$ over three months, and the plants were allowed to grow freely. When the plants were well established and the constructed wetlands stabilized, the investigation commenced. The influent flow to the wetlands system was set to $0.6 \text{ m}^3 \text{ days}^{-1}$, corresponding to a theoretical hydraulic retention time of 21 days, based on the actual hydraulic retention time of Yanlong Lake of approximately 21 days and 10 hours

(Xu *et al.* 2019). There were four sampling points at the entrance and exit of each wetland, as shown in Figure 1. All data in this study were collected in April 2018.

Procedure of DOM fractionation

DOM from the sampling points was separated into three chemical fractions, HPO, transphilic (TPI), and HPI fractions, using Amberlite XAD-8/XAD-4 resin chromatography developed by Leenheer (1981) and Aiken *et al.* (1992); a schematic of this experimental step is presented in Figure 2(a). In order to avoid the loss of DOC during resin enrichment and elution, the quantitative method from Imai *et al.* (2001) and Wei *et al.* (2008) was adopted. First, $0.45 \mu\text{m}$ filtered water samples were adjusted to pH 2 with HCl and pumped through a glass column containing Amberlite XAD-8 resin. The effluent from this glass column was the TPI and HPI fractions, while the HPO fraction was retained on the resin. This HPO fraction contained most of the humic substances and could be eluted with 0.1 mol L^{-1} NaOH. After desorption of the HPO

Table 1 | Water quality parameters of raw water from the Viper River ($n = 12$)

Parameter	Unit	Range	Mean \pm SD
pH	–	7.45–7.99	7.64 ± 0.14
Br^-	mg L^{-1}	0.19–0.40	0.29 ± 0.07
COD_{Mn}	mg L^{-1}	4.60–7.10	5.98 ± 0.92
Ammonium nitrogen	mg L^{-1}	0.22–1.19	0.56 ± 0.26
Total nitrogen	mg L^{-1}	1.50–3.14	2.67 ± 0.46
Total phosphorus	mg L^{-1}	0.04–0.23	0.14 ± 0.06
UV_{254}	cm^{-1}	0.08–0.17	0.10 ± 0.03
TOC	mg L^{-1}	8.29–14.23	10.84 ± 1.60

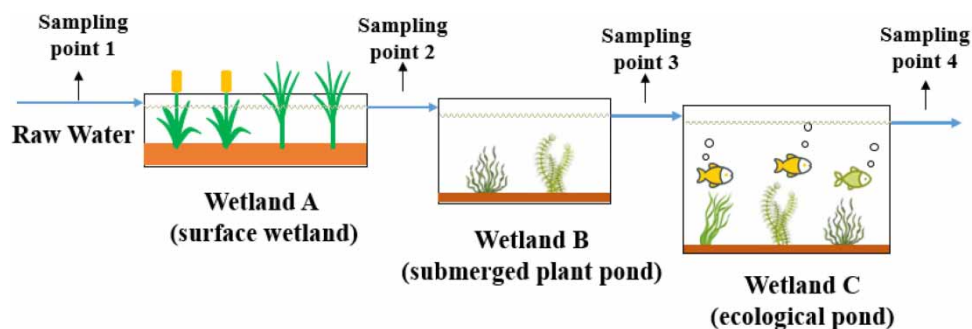
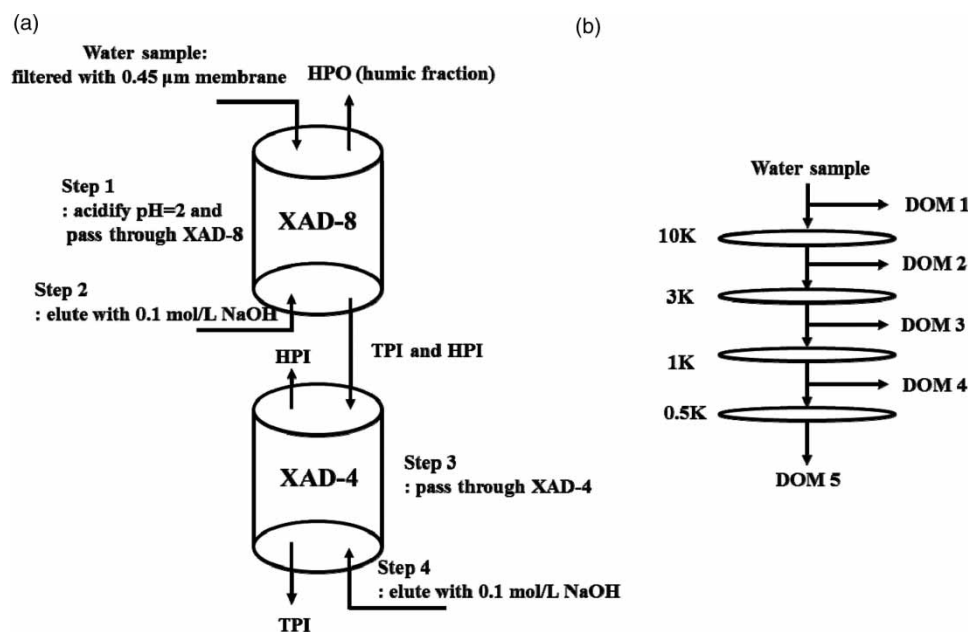


Figure 1 | A schematic diagram of the pilot-scale constructed wetlands.

Table 2 | Wetlands system parameters and installation composition

Name	Size/mm	Maximum depth of the water/m	Plant species	Number	Matrix type	Matrix thickness/m
Wetland A	2,650 × 800 × 600 × 15	0.2	Cattail, <i>Zizania aquatica</i>	2	River sand	0.3
Wetland B	2,500 × 1,350 × 1,000 × 15	0.8	Valerian, goldfish	1	Soil	0.05
Wetland C	3,800 × 1,600 × 1,700 × 15	1.5	Valerian, goldfish, spirulina	1	Soil	0.05

**Figure 2** | Schematic diagrams of the procedures for DOM fractionation. (a) Fractionation of DOM by resin adsorption; (b) fractionation of DOM by ultrafiltration.

fraction, the effluent from the XAD-8 resin containing HPI acids, bases, and neutral compounds was then passed through the XAD-4 resin. The TPI fraction was obtained by eluting the XAD-4 resin with the same eluent used to wash the XAD-8 resin. The soluble organics passing through the XAD-4 resin were the HPI fraction, containing HPI bases and neutral compounds (not retained on either the XAD-8 or XAD-4 resin). All separated water samples were adjusted to pH 7.0 (± 0.2) using HCl or NaOH.

Another set of water samples was fractionated to different molecular weight classes using a stirred ultrafiltration cell (Millipore, 8400) with YM disc membranes (Amicon, nominal molecular weight cut-offs are 0.5, 1, 3 and 10 kDa). All membranes were rinsed with ultrapure water to ensure a residual DOC concentration of $<0.2 \text{ mg}\cdot\text{L}^{-1}$. The DOC mass balance of our size fractionation had been

controlled in $(100 \pm 5)\%$ following the cleaning procedure used by Guo & Santschi (1996) and Wei et al. (2008). A schematic of the specific separation steps is presented in Figure 2(b). Then, DOC, UV_{254} , and DBPFP were measured for all fractionated samples.

DOM and DBPFP measurements

A total of five water samples were collected in pre-cleaned 250 mL glass bottles at each sampling location on the sampling date in April 2018. The samples were then mixed in a larger bottle and cooled immediately in an ice cooler. After filtration through a $0.45 \mu\text{m}$ cellulose membrane filter, the raw water and wetland effluent samples were stored in a dark room at 4°C to minimize changes in the constituents. When ready for analysis, the samples were

removed from this environment, and the DOC was measured using a high-temperature combustion method, based on Standard Method 5310B, using the OI Analytical Aurora 1030 W Total Organic Carbon Analyzer equipped with an auto-sampler.

UV₂₅₄ was performed with a spectrophotometer (Thermo scientific corporation, EVOLUTION201, USA) using a 1 cm quartz cell. Specific UV₂₅₄ (SUVA) was calculated by dividing the UV₂₅₄ measurement by the DOC concentration.

DBPFP measurements were performed using a modified version of Standard Method 5710B. Fractionated samples of 250 mL at 20 ± 2 °C in amber bottles containing PTFE liners were buffered with 0.05 mol L⁻¹ phosphate to a pH of 7 ± 0.2, and then 750 µL NaOCl were added. The samples were left to react for three days, and then the residual free chlorine was measured using a chlorine residual pocket colorimeter. If samples were found to have a residual free chlorine level of between 3 and 5 mg L⁻¹, the residual chlorine was immediately quenched with ascorbic acid (Hach Company, PCII, USA). THM and HAA analyses were then conducted immediately. The concentrations of THMs (trichloromethane (TCM),

bromodichloromethane (BDCM), dibromochloromethane (DBCM) and tribromomethane (TBM)) were measured by liquid/liquid extraction with methyl-tertiary-butyl-ether using the Agilent GC-7890B gas chromatograph based on USEPA Method 551.1. Similarly, HAAs (monochloroacetic acid (MCAA), dichloroacetic acid (DCAA), trichloroacetic acid (TCAA), monobromoacetic acid (MBAA), dibromoacetic acid (DBAA)) were analyzed using gas chromatography–electron capture detection with methyl-tertiary-butyl-ether and derivatization with acidic methanol, according to USEPA Method 552.2. The full names and abbreviations of related terms are shown in Table 3.

RESULTS AND DISCUSSION

Fraction distributions of the DOM

The molecular weight distributions of DOM in raw water and wetland effluents are presented in Figure 3(a). The low molecular weight fraction (<3 kDa) of DOM generally

Table 3 | Glossary of terms

Term	Definition	Term	Definition
BDCM	Bromodichloromethane	HRT	Hydraulic retention time
C-DBPs	Carbonaceous disinfection by-products	MBAA	Monobromoacetic acid
DBAA	Dibromoacetic acid	MCAA	Monochloroacetic acid
DBAAFP	Dibromoacetic acid formation potential	MTBE	Methyl-tertiary-butyl-ether
DBCM	Dibromochloromethane	N-DBPs	Nitrogenous disinfection by-products
DBPs	Disinfection by-products	RA	Resin adsorption
DBPFP	Disinfection by-products formation potential	SDBPFP	Special-Specific DBPFP
DCAA	Dichloroacetic acid	SHAAFP	Special-Specific-HAAFP
DCAAFP	Dichloroacetic acid formation potential	SMPs	Soluble microbial products
DOC	Dissolved organic carbon	STHMFP	Specific THMFP
DOM	Dissolved organic matter	TBM	Tribromomethane
HAAFP	Haloacetic acids formation potential	TCM	Trichloromethane
HAAs	Haloacetic acids	TCAA	Trichloroacetic acid
HPI	Hydrophilic	THAAFP	Total HAAFP
HPIB	Hydrophilic bases	THMs	Trihalomethanes
HPO	Hydrophobic	THMFP	Trihalomethanes formation potential
HPOA	Hydrophobic acid	TPI	Transphilic
HPOB	Hydrophobic bases	TTHMFP	Total THMFP
HPON	Hydrophobic neutrals		

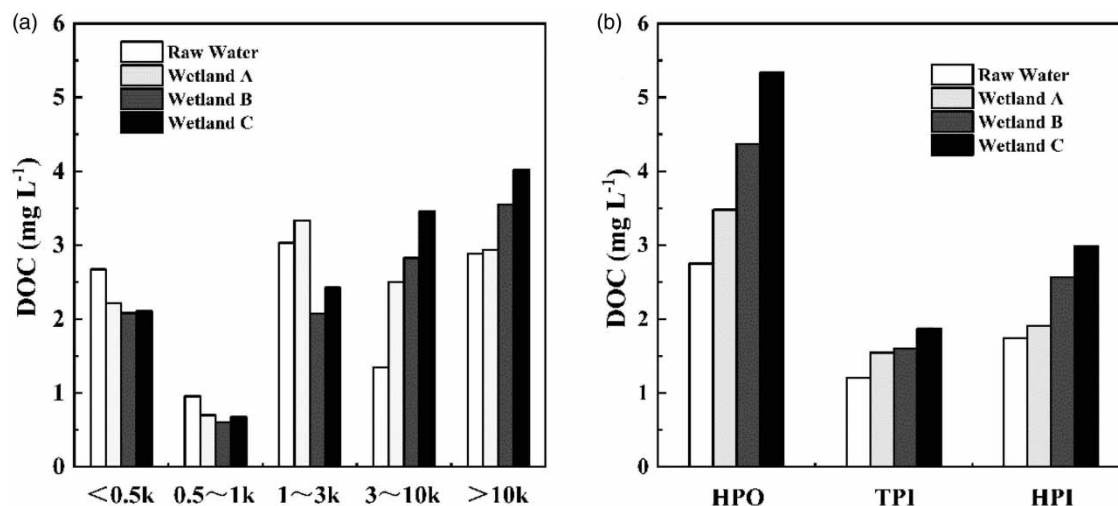


Figure 3 | DOC for DOM and its fractions in raw water and constructed wetland effluents. (a) DOC for size fractions; (b) DOC for chemical fractions.

showed a decreasing trend along the water path, whereas the higher molecular weight fraction (>3 kDa) exhibited the opposite trend, indicating that the constructed wetland system reduces low molecular weight DOM but concentrates high molecular weight DOM. Similarly, a previous study (Guo *et al.* 2012) indicated that biological treatment can effectively remove organics with a low molecular weight (<1 kDa) while increasing the proportion of DOM with a higher molecular weight (>10 kDa). Microbial degradation and assimilation may play key roles in this process. Biodegradable small-molecule organic matter is decomposed into H₂O and CO₂ and other small molecules (CH₄, N₂, NH₃) under the action of microorganisms, thus escaping the wetland ecosystem. Furthermore, assimilation by microorganisms transforms HPI small-molecule organic matter (such as amino acids and ribose) into large-molecule cellular material, which reduces the concentrations of small-molecule organic matter in the water. Assimilation by microorganisms can also explain the increase in concentration of large molecular weight organic matter, as extracellular secretions of microorganisms are mostly macromolecular organic substances (Yang *et al.* 2016).

As shown in Figure 3(b), the distributions of all DOM chemical fractions increased along the water path, with the largest variation observed for the HPO fraction (94% increased DOC in the effluent). These results are not consistent with the study conducted by Wei *et al.* (2008), which concluded that the HPO/HPI (especially HPI) character

of DOM from secondary effluents decreased significantly with horizontal subsurface flow through a wetland treatment system. The dominant component in raw water and all wetland effluents was the HPO fraction, accounting for approximately 50% of the DOC content; results from other studies have indicated that the HPI fraction forms the largest proportion of DOM in water sources (Marhaba & Van 2000; Kitis *et al.* 2002). However, it has been widely documented that the HPO fraction, mainly humic acid and fulvic acid macromolecular substances, is the main precursor of DBPs (Hanigan *et al.* 2013).

UV₂₅₄ and specific ultraviolet absorbance (SUVA)

The UV₂₅₄ value is often used in the water industry as a surrogate parameter to estimate the yields of THM precursors in source waters. Figure 4(a) and 4(b) show the UV₂₅₄ values obtained using the two classification methods (molecular weight fractionation and chemical fractionation) from raw water at the three different wetlands. A similar relationship between DOC and UV₂₅₄ was observed for all water samples in this study, and for all size and chemical fractions, except the TPI fraction. The highest DOC and UV₂₅₄ values were observed in the 3–10 kDa weight fraction, with a UV₂₅₄ of 0.053 cm⁻¹ and DOC level of 2.25 mg L⁻¹. The 3–10 kDa fraction has been found to dominate the UV₂₅₄ composition in other source waters, such as the Miyun reservoir in Beijing, the Huanghe River in Tianjing, the Pearl River in

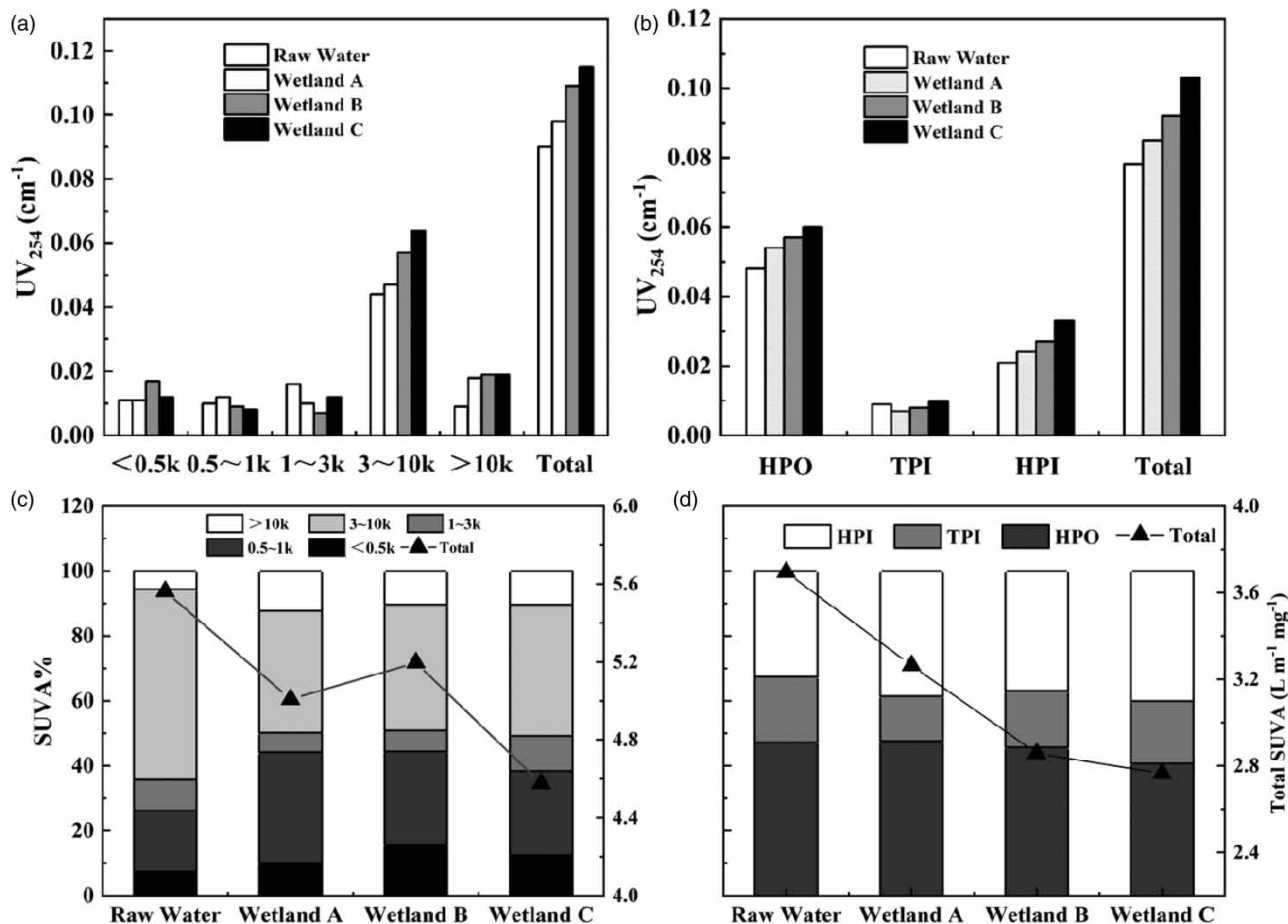


Figure 4 | UV_{254} for DOM and its fractions in raw water and constructed wetland effluents. (a) and (c) DOC for size fractions; (b) and (d) DOC for chemical fractions.

Guangzhou, and the East-Lake reservoir in Shenzhen (Wei *et al.* 2008). The values for the other molecular weight fractions were much lower. The HPO fraction was the predominant constituent ($\sim 60\%$) in the UV_{254} results among the chemical fractions (Figure 4(b)), which may be because this fraction forms the largest proportion of the DOC content ($\sim 50\%$) (Figure 3(b)). It has also been reported in previous studies that simple and reliable relationships exist between the change in the DOC UV absorbance when it is chlorinated and the formation of chlorinated byproducts (Li *et al.* 2000).

The specific ultraviolet absorbance is a useful parameter for estimating the dissolved aromatic carbon content in aquatic systems (Weishaar *et al.* 2003). Figure 4(c) and 4(d) present the SUVA% and total SUVA of samples. Within the two classification methods, the molecular weight fraction of

3–10 kDa and the HPO chemical fraction accounted for approximately 40 and 45%, respectively, of the total SUVA in each type of water sample, similar to the UV_{254} and DOC distributions. Interestingly, the total UV_{254} increased along the water path in the pilot plant, while the total SUVA decreased. A previous study (Li *et al.* 2008) showed that influent DOM consists of relatively unstable alcohol and olefins, in contrast to stable aromatics and alkyl hydrocarbons in the effluent, indicating that the SUVA of the effluent will be higher than that of the influent. This is inconsistent with our results, possibly due to differences in influent water quality, the plant environment, and the matrices used in the experiments, or regional differences in water sources and the proportions of different components. Hua & Reckhow (2007) reported that water with higher SUVA values typically contains more HPO carbon and polyhydroxy

components, and that the aromatic structure present in HPO substances is the main precursor of THMs (Rook 1976). Therefore, the SUVA results showed that the wetland treatments increased the quality of aromatic materials but decreased the aromaticity, which may reduce the DBP level produced per unit mass.

Size and chemical fractions of DBPFP

The THMFP and HAA formation potential (HAAFP) are often employed to indicate the concentrations of THMs and HAAs

that can be produced during the chlorination process and can indirectly represent the amounts of THM precursors in water samples. As shown in Figures 5 and 7, the THMFP and HAAFP tests were used to evaluate one aspect of THM and HAA formation resulting from a precursor. The total THMFP (TTHMFP) was calculated as the sum of the formation potentials of TCM (TCMFP), BDCM (BDCMFP), DBCM (DBCMFP), and TBM (TBMFP). Similarly, the total HAAFP (THAAFP) was calculated as the sum of the formation potentials of TCAA (TCAAFF), DCAA (DCAAFF), DBAA (DBAAFF), MCAA (MCAAFF), and MBAA.

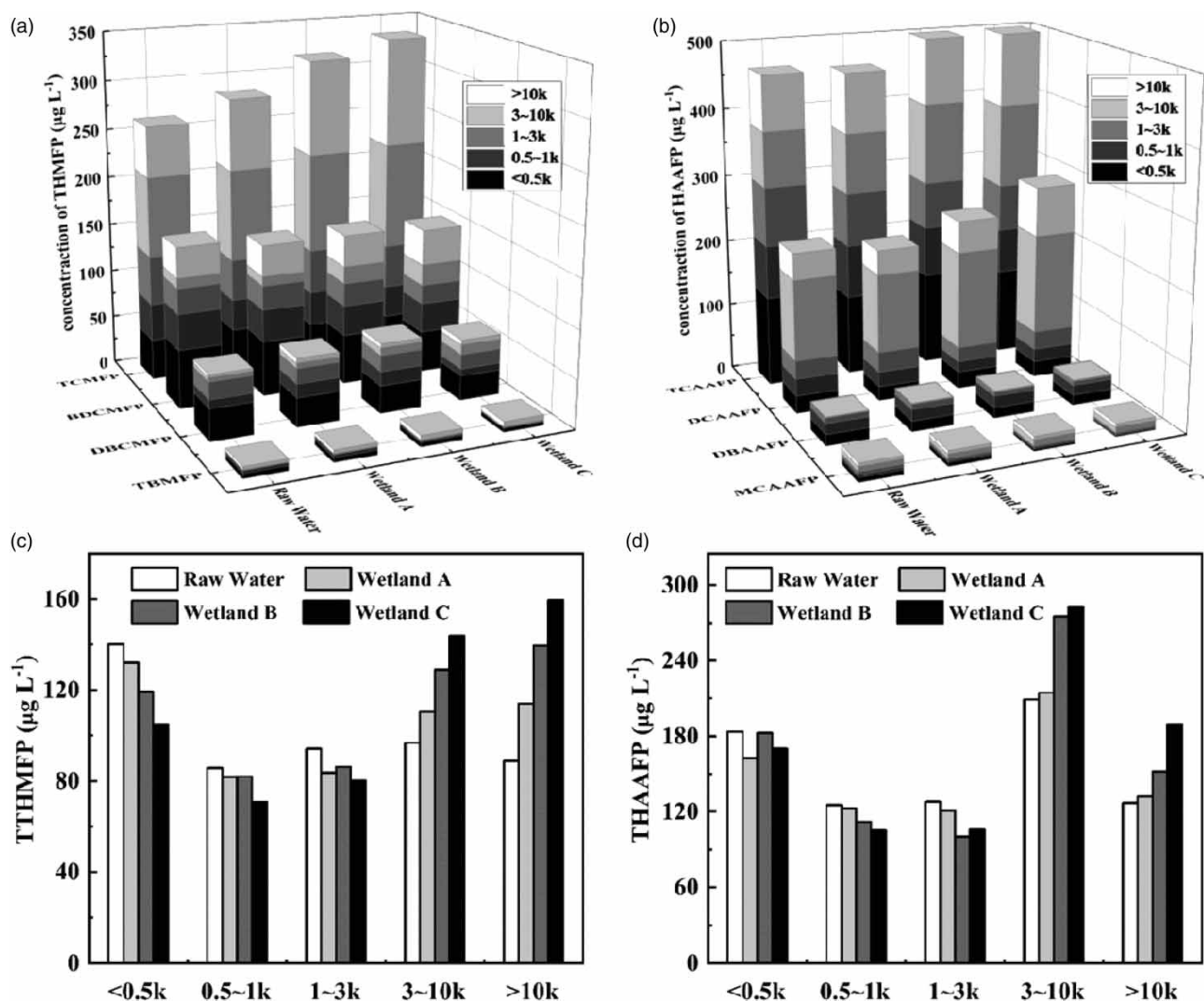


Figure 5 | THMFP and HAAFP for the DOM and its size fractions in raw water and wetland effluents. (a) and (b) THMFP and HAAFP distribution of molecular weight size fractions; (c) and (d) total THMFP and HAAFP of each molecular weight size fraction.

Size fractions of DBPFP

Among all water samples, TCMFP had the highest average contribution to the THMFP in the raw water and the three types of wetland effluent, whereas TBMFP had the lowest (Figure 5(a)). More than 30% of the bromo-THM species (DBCMFP, BDCMFP, and TBMFP) formed by chlorination were converted in the <0.5 kDa fraction of DOM; more than 58% of bromo-THM species were accumulated in the <1 kDa fraction. Similar results have been observed in previous studies, which demonstrated that the contribution of bromo-THM species to the TTHMFP was higher than that of chloroform in the <1 kDa fraction (Xu *et al.* 2007). Conversely, unlike in other fractions, TCMFP with a molecular weight of 3–10 kDa is the most abundant (~32.5%) among all molecular weight fractions. It can be deduced that the contribution of bromo-THM species to the TTHMFP was higher than that of TCM for the smallest fractions, but the contribution of TCM to the TTHMFP was higher than that of bromo-THM for the larger fractions, mainly due to the lower concentration of bromide compared with chlorine (Kitis *et al.* 2010). The TTHMFP does not differ greatly among the five molecular weight fractions; however, the specific THMFP (STHMFP, THMFP/DOC) in the <1 kDa fraction, especially the 0.5–1 kDa fraction, was more than two times greater than that in the >1 kDa fraction, as shown in Figure 6. Despite the large amount of organic fractions, which may result in the formation of more THMs

during the chlorination process, the specific DBPFP (SDBPFP, DBPFP/DOC) of such organic fractions may not follow the same trend. In general, the larger fractions are usually more aliphatic, whereas smaller fractions are more aromatic with higher numbers of carboxyl groups (Li *et al.* 2014), so components with smaller molecular weights are more likely to form THMs during chlorine disinfection. In summary, in the five molecular weight fractions: (1) the <1 kDa fraction was the primary source of bromo-THMFP, and the >3 kDa fraction was the primary source of chloro-THMFP; (2) the TTHMFP concentration did not differ greatly among the five fractions, but the STHMFP was much higher in the <1 kDa fraction than in the other fractions.

The HAAFP values for each DOM molecular weight range in raw water and wetland effluents are shown in Figure 5(b). Only five HAA substances were analyzed in the water sample after chlorination, namely MCAA, MBAA (not shown in Figure 5(b) because the concentration is too low), DCAA, DBAA, and TCAA. The concentration of chloroacetic acid was significantly higher compared with that of bromoacetic acid, and the HAAFP was generated mostly from the TCAA precursor, followed by, in decreasing order, the precursors of DCAA, DBAA, MCAA, and MBAA. The same association with the size fraction observed with THMFP was seen for HAAFP. For DCAAFP (chloro-HAAFP), the highest DCAAFP yields occurred in the 3–10 kDa fraction, while the fraction with a molecular weight <1 kDa yielded the highest bromo-HAAFP

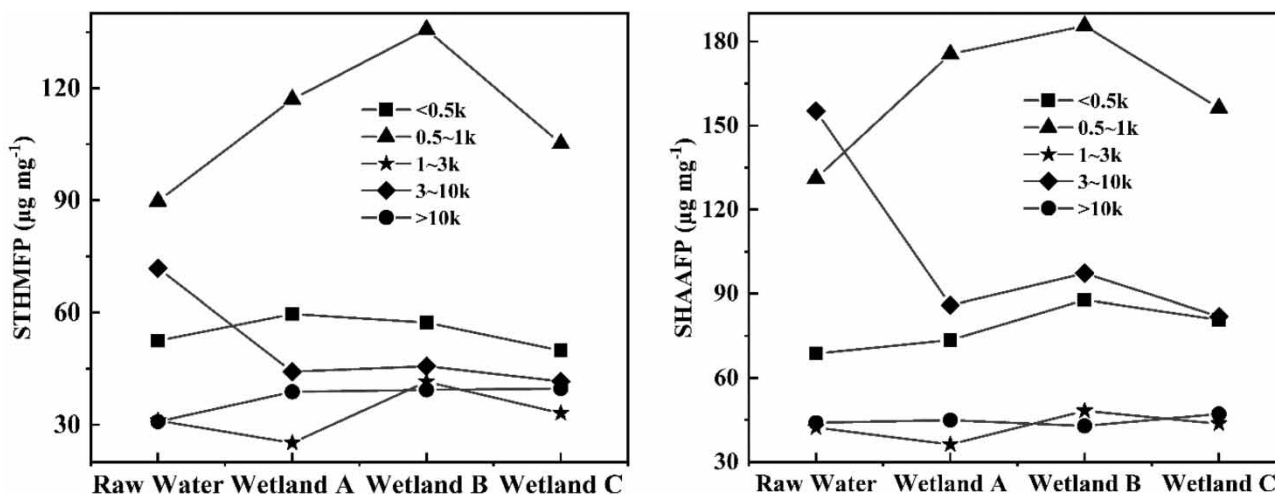


Figure 6 | STHMFP and SHAAFP of each size fraction along the water path.

(DBAAFP), accounting for approximately 75% of all fractions. It can be seen in Figure 5(d) that the THAAFP was highest in the 3–10 kDa fraction, and the HAAFP was almost the same between the <3 kDa and >3 kDa fractions. However, the average specific HAAFP (SHAAFP, HAAFP/DOC) values of the different molecular weight fractions were 77.06, 158.70, 41.87, 96.94, and 44.88 $\mu\text{g mg}^{-1}$ in the <0.5, 0.5–1, 1–3, 3–10, and >10 kDa fractions, respectively. Kitis *et al.* (2002) isolated DOM from surface waters and found that the 1–3 kDa fraction produced the highest HAA yield. However, other studies (Hua & Reckhow 2007; Xu *et al.* 2007) have demonstrated that HAAs are generated from high molecular weight fractions in surface waters, particularly components with a molecular weight >3 kDa. These conclusions differ from our results, and this observation may be applicable to DCAAFP but less applicable to the other HAAFP species investigated in this work. Source-related environmental conditions may be the main reason for the difference in results. Our results for HAAFP are consistent with those for THMFP and support the view that the low molecular weight fractions, especially molecular weights <3 kDa, are the primary source of THM and THAA precursors in natural waters.

As shown in Figure 5(c) and 5(d), the TTHMFP and THAAFP of DOM did not change significantly before and after wetland treatment, but the contribution of DOM in different molecular weight fractions to the THMFP and HAAFP varied greatly. More specifically, the contribution of DOM in the <3 kDa fraction to the THMFP and HAAFP decreased along the water path, while the contribution of DOM in the >3 kDa fraction increased. A similar trend for DBPFP and DOC was observed across the molecular weight distribution of DOM, while there was no strong correlation between the DOM molecular weight distribution and SUVA or STHMFP.

The increased DOC in the process of constructed wetland treatment mainly comes from the 3~10 kDa fractions, which may come from the secretion of plant roots or the degradation of microorganisms. The SDBPFP of the increased part of the DOC is relatively low, so the SDBPFP of the effluent is reduced. We believe that the 0.5–1 kDa component is mainly derived from micro-polluted raw water. This part of DOC may be a product of human activities, and DBPFP is higher. The wetland

treatment process does not generate this part of DOC, so there is almost no change in the wetland treatment process.

Chemical fractions of DBPFP

The THMFP and HAAFP of the HPI/HPO fractions of raw water and the three types of wetland effluent are shown in Figure 7. For THMFP contributions, as shown in Figure 7(a), the highest THMFP concentration of 299.35 $\mu\text{g L}^{-1}$ was detected in the effluent of wetland C, and the order of the THMFP contributions was TCMFP > BDCMFP > DBCMFP > TBMFP. Bromo-THM (BDCM, DBCM, and TBM) accounted for more than 40% of the TTHMFP in the wetland system, which may be due to the Br concentration in the system influent. There is a large area of saline-alkali tidal flat in Yancheng, close to the Yellow Sea, and seawater intrusion and pollution from the salinization industry will lead to high Br concentrations in surface water. Related studies (Uyak & Toroz 2007) have shown that when the organic matter content in the raw water is constant, the proportion of brominated DBPs increases with the Br concentration. The two main THM precursors in the sampling water were found to be HPO and HPI (42.3% and 38.7% by weight on average, respectively). However, the HPI/HPO nature of the DBP precursors has an effect on the THM species formed, and more than 50% of the chloro-THM species formed by chlorination were converted from the HPO fraction of DOM. In contrast, more than half of the bromo-THM species formed by chlorination were converted from the HPI fraction of DOM. In other words, the HPO and HPI fractions were the main sources of chloro-THMFP and bromo-THMFP, respectively. The same effect has been found in previous studies (Xu *et al.* 2007), demonstrating that the contribution of bromo-THM species to the TTHMFP was higher than that of chloroform in the non-acid HPI fractions.

Figure 7(b) shows the concentrations of the four HAAFP species in each chemical fraction after wetland treatment. The DOM in raw water and wetland effluents exhibited contrasting HAAFP values, ranking in the following order: TCAAFF > DCAAFF > DBAAFF > MCAAFF. The TCAAFF accounted for almost 60% of the THAAFP. The HPO fraction from DOM in raw water and wetland effluents is the main precursor of HAAs; however, the HPI fraction

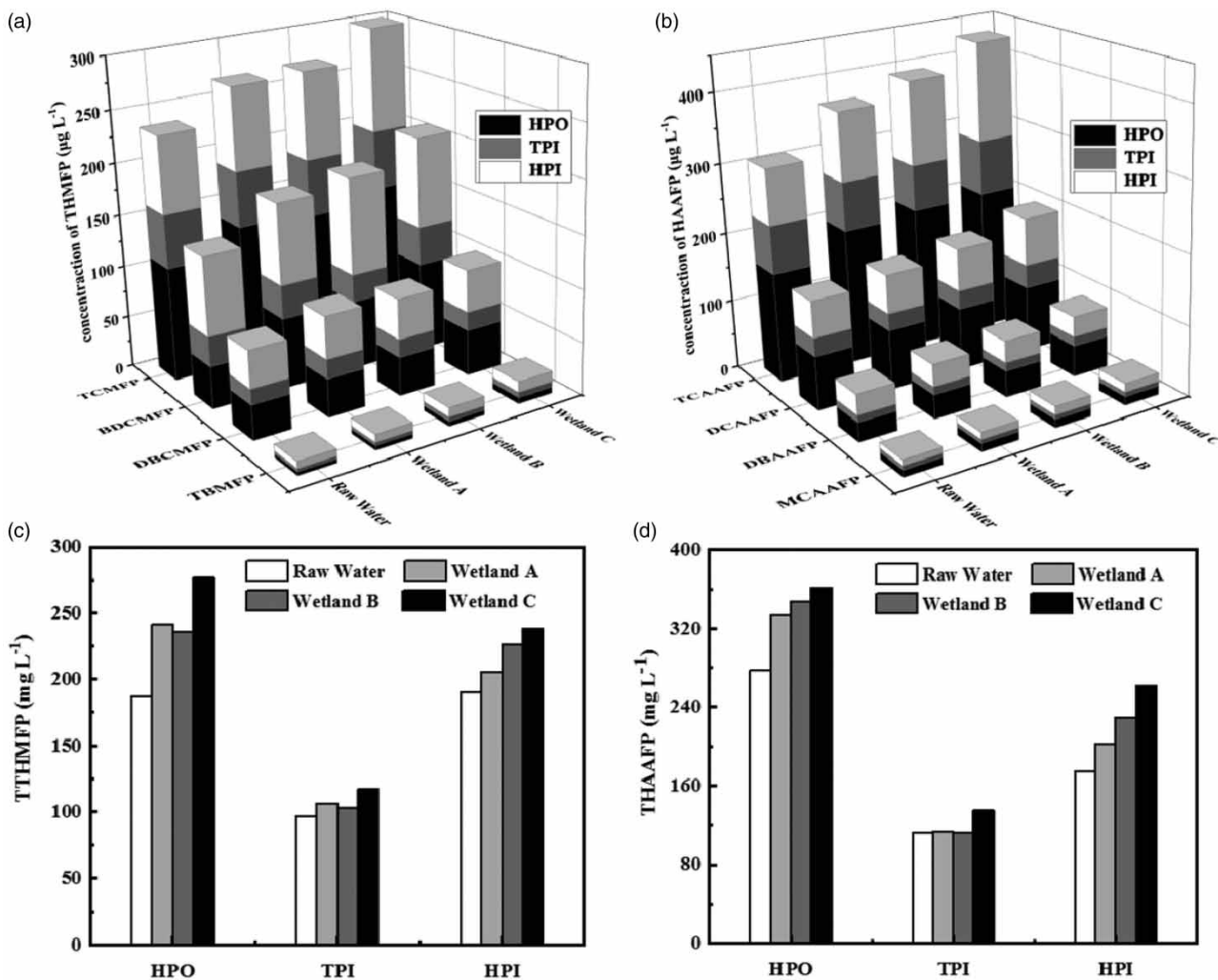


Figure 7 | THMFP and THAAFP for the DOM and its chemical fractions in raw water and wetland effluents. (a) and (b) THMFP and HAAFP distribution for chemical fractions; (c) and (d) total THMFP and HAAFP for chemical fractions.

also exhibits a high HAAFP. HPO organic matter is mainly humic acid, and weakly HPO organic matter is composed mainly of fulvic acid; HPI organic matter contains some small molecular organic compounds with low carbon-containing single bonds and aromatic structures, such as polysaccharides, proteins, and amino acids (Amery *et al.* 2009). Moreover, humus contains a large number of carbon-carbon double bonds and aromatic rings with high halogen activity, which can react rapidly with chlorine to form a large number of DBPs (Kanokkantung *et al.* 2006). Therefore, HPO components exhibited a higher DBPFP value.

Kraus *et al.* (2008) evaluated the effects of wetlands on the formation of DBPs in the Sacramento–San Joaquin Delta and found that the THMFP and HAAFP increased

by 1–3.3 times and 1.2–4.3 times after wetland treatment, respectively. Similar research conclusions were drawn here (Figure 7(c) and 7(d)). The TTHMFP along the water path increased from 474.41 to 631.68 $\mu\text{g L}^{-1}$, yielding a relatively higher production efficiency of 33.15% compared with the raw water. As may be expected, the THAAFP trend was almost consistent with this. Among the three chemical fractions, the change in the HPO fraction was the largest, with a THMFP value approximately 47.68% higher than that in raw water, whereas the HAAFP of the HPI fraction was 1.5 times higher. It is likely that in the process of treating the source water through the wetland ecosystem, the extracellular secretions produced by algae, root exudates secreted by plants, or animal metabolites increase the

DBPFP of wetland effluents. The DOC, UV₂₅₄, TTHMFP and THAAFP of HPO and TPI fractions in constructed wetland effluent increased significantly, while the TPI fractions along the water path hardly changed. Compared with influent samples, the increase rates of DOC, UV₂₅₄, TTHMFP and THAAFP of HPO in wetland effluent samples were 93.9%, 25%, 47.7% and 30.3%, respectively. And the corresponding increase in HPI was 70.8%, 32.1%, 25.1% and 50.1%. We suspect that this was caused by the NOM secreted by plant roots and algae in the wetland, but further investigation is needed.

All of the DOM fractions exhibited decreased STHMFP and SHAAFP during wetland treatment, corresponding to a decrease in the SUVA (Figure 8). The average STHMFP values in the three chemical fractions were 60.83, 68.90, and 96.24 $\mu\text{g mg}^{-1}$ for the HPO, TPI, and HPI fractions, respectively. The SDBPFP of the small molecule fractions (<1 kDa) and the HPI fractions are both the highest. It can be considered that the main fractions of the small molecule component is HPO, which are the main DBPs precursors for the effluent of the constructed wetland. The same general trend was observed for the SHAAFP with respect to the different chemical fractions. Although the HPO fraction was dominant at all stages of wetland treatment, the SDBPFP was higher in the HPI than HPO fractions. HPO fractions are composed of HPO acids (consisting of five- to nine-carbon aliphatic carboxylic acids, one- and two-ring aromatic carboxylic acids, aromatic

acids, etc.), HPO bases (consisting of proteins, high molecular weight alkyls, etc.), and HPO neutrals (HPON, consisted of aliphatic alcohols, alkyl alcohols, ethers, ketones, aldehydes, etc.) (Kanokkantapong *et al.* 2006). According to previous reports (Krasner & Amy 1995), HPON contain a considerable amount of ash and therefore a low carbon content compared with other HPO fractions, the organic matter of HPON may not form DBPs so readily. If the HPO fraction has a high HPON content, then this would explain why the SDBPFP of the HPO fraction is very low. In contrast, the SDBPFP of the HPI fraction was extraordinarily high at 95.99 $\mu\text{g mg}^{-1}$ on average (STHMFP and SHAAFP: 96.24 and 95.74 $\mu\text{g mg}^{-1}$, respectively). A similar conclusion has been observed in other studies (Kanokkantapong *et al.* 2006) for SHAAFP, with a SHAAFP of 139.31 $\mu\text{g mg}^{-1}$ observed for HPI bases (consisting of aliphatic amines with less than nine carbons, amino acids, pyridines, etc.). Thus, HPI bases are considered the most active HPI species in the chlorination reaction.

Furthermore, although TTHMFP and THAAFP of each chemical fraction along the water path increased, the STHMFP and SHAAFP decreased in accordance with the decrease in the SUVA as a result of wetland treatment. This indicated that the DBPFP of DOM generated in the wetlands is smaller than that of the raw water. In other words, our findings implied that the DOM produced by the constructed wetland system may not readily generate DBPs during chlorination.

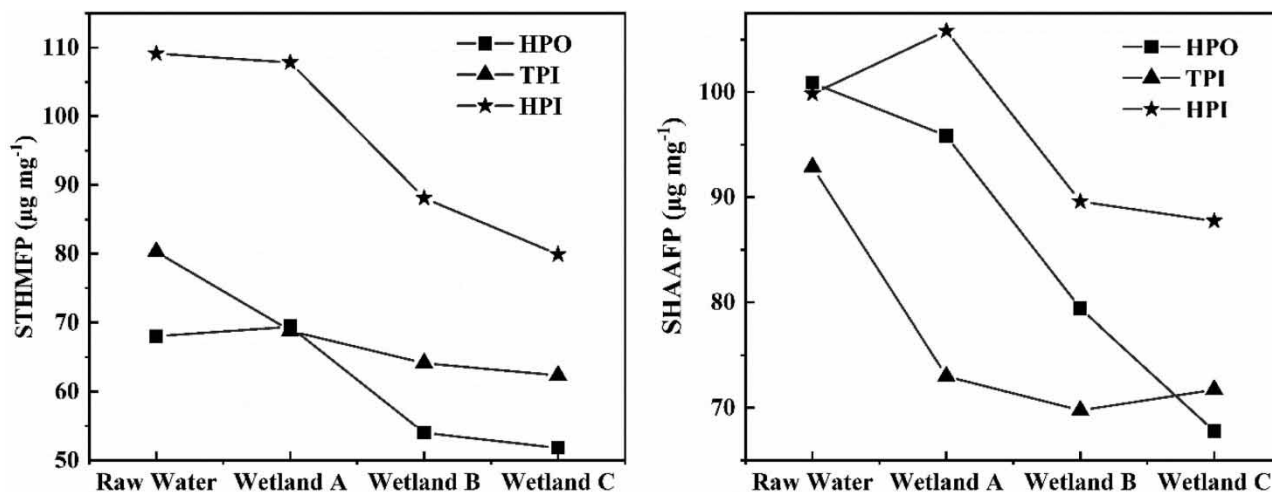


Figure 8 | STHMFP and SHAAFP of each chemical fraction along the water path.

CONCLUSIONS

The following conclusions are supported by our experimental results:

- (1) The low molecular weight fraction (<3 kDa) of DOC and DBPFP generally showed a decreasing trend along the water path, whereas the large molecular weight fraction (>3 kDa) exhibited an increasing trend, which may be related to the transformation and degradation of DOM by microorganisms in wetlands and the characteristics of exudates secreted by the root systems of wetland plants.
- (2) The <1 kDa fraction was the primary source of bromo-THMFP, and the >3 kDa fraction was the primary source of chloro-THMFP. Additionally, the <1 kDa fractions showed much higher SDBPFP than that of the other fractions, indicating that smaller molecular weight DOM has a greater potential for generating DBPs.
- (3) Compared with raw water, DOC, UV₂₅₄, and DBPFP in the treated wetland effluents increased. However, all of the chemical DOM fractions exhibited decreased SDBPFP in accordance with the decrease in the SUVA during wetland treatment. This indicates that the increased concentrations of DBP precursors in the wetland system may be less readily chlorinated to generate DBPs.
- (4) Although the HPO fraction was the most abundant at all stages of wetland treatment, the SDBPFP of the HPI fraction was higher than that of the HPO fraction.

ACKNOWLEDGEMENTS

This study was supported by the Natural Science Foundation of Jiangsu Province (BK20191147) and the Major Science and Technology Program for Water Pollution Control and Treatment (2014ZX07405002).

DATA AVAILABILITY STATEMENT

All relevant data are included in the paper or its Supplementary Information.

REFERENCES

- Aiken, G. R., McKnight, D. M., Thorn, K. A. & Thurman, E. M. 1992 Isolation of hydrophilic organic acids from water using nonionic macroporous resins. *Org. Geochem.* **18** (4), 567–573.
- Amery, F., Vanmoorleghem, C. & Smolders, E. 2009 Adapted DAX-8 fractionation method for dissolved organic matter (DOM) from soils: development, calibration with test components and application to contrasting soil solutions. *Eur. J. Soil Sci.* **60** (6), 956–965.
- Cheng, W., Dastgheib, S. A. & Karanfil, T. 2005 Adsorption of dissolved natural organic matter by modified activated carbons. *Water Res.* **39** (11), 2281–2290.
- Dierberg, F. E., DeBusk, T. A., Jackson, S. D., Chimney, M. J. & Pietro, K. 2002 Submerged aquatic vegetation-based treatment wetlands for removing phosphorus from agricultural runoff: response to hydraulic and nutrient loading. *Water Res.* **36** (6), 1409–1422.
- Guo, L. & Santschi, P. H. 1996 A critical evaluation of cross-flow ultrafiltration technique for sampling colloidal organic carbon in seawater. *Mar Chem.* **55** (1–2), 113–127.
- Guo, J., Sheng, F., Guo, J., Yang, X., Ma, M. & Peng, Y. 2012 Characterization of the dissolved organic matter in sewage effluent of sequence batch reactor: the impact of carbon source. *Front. Env. Sci. Eng.* **6** (2), 280–287.
- Hanigan, D., Inniss, E. & Clevenger, T. E. 2013 MIEX[®] and PAC for removal of hydrophilic DBP precursors. *J. Am. Water Works Ass.* **105** (3), 41–42.
- Hansen, A. M., Kraus, T. E. C., Bachand, S. M., Horwath, W. R. & Bachand, P. A. M. 2018 Wetlands receiving water treated with coagulants improve water quality by removing dissolved organic carbon and disinfection byproduct precursors. *Sci. Total Environ.* **622–623**, 603–613.
- Haynes, R. J. 2015 Use of industrial wastes as media in constructed wetlands and filter beds-prospects for removal of phosphate and metals from wastewater streams. *Crit. Rev. Env. Sci. Tech.* **45** (10), 1041–1103.
- Hinsinger, P., Plassard, C. & Jaillard, B. 2006 Rhizosphere: a new frontier for soil biogeochemistry. *J. Geochem. Explor.* **88** (1–3), 210–213.
- Hua, G. & Reckhow, D. A. 2007 Characterization of disinfection byproduct precursors based on hydrophobicity and molecular size. *Environ. Sci. Technol.* **41** (9), 3309–3315.
- Huang, J. 2000 Nitrogen removal in constructed wetlands employed to treat domestic wastewater. *Water Res.* **34** (9), 2582–2588.
- Iamchaturapatr, J., Yi, S. W. & Rhee, J. S. 2007 Nutrient removals by 21 aquatic plants for vertical free surface-flow (VFS) constructed wetland. *Ecol. Eng.* **29** (3), 287–293.
- Imai, A., Fukushima, T., Matsushige, K. & Kim, Y. H. 2001 Fractionation and Characterization of dissolved organic matter in a Shallow Eutrophic lake, its inflowing rivers, and other organic matter sources. *Water Res.* **35** (17), 4019–4028.
- Kanokkantapong, V., Marhaba, T. F., Pavasant, P. & Panyapinyophol, B. 2006 Characterization of haloacetic acid precursors in source water. *J. Environ. Manage.* **80** (3), 214–221.

- Kitis, M., Karanfil, T., Wigton, A. & Kilduff, J. E. 2002 Probing reactivity of dissolved organic matter for disinfection by-product formation using XAD-8 resin adsorption and ultrafiltration fractionation. *Water Res.* **36** (15), 3834–3848.
- Kitis, M., Yigita, N. O., Harmana, B. I., Muhammetoglu, H., Muhammetoglu, A., Karadirek, I. E., Demirel, I., Ozdenc, T. & Palancic, I. 2010 Occurrence of trihalomethanes in chlorinated groundwaters with very low natural organic matter and bromide concentrations. *Environ. Forensics* **11** (3), 264–274.
- Krasner, S. W. & Amy, G. 1995 Jar-test evaluations of enhanced coagulation. *J. Am. Water Works Ass.* **87** (10), 93–107.
- Kraus, T. E. C., Bergamaschi, B. A., Hernes, P. J., Spencer, R. G. M., Stepanauskas, R., Kendall, C., Losee, R. F. & Fujii, R. 2008 Assessing the contribution of wetlands and subsided islands to dissolved organic matter and disinfection byproduct precursors in the Sacramento-San Joaquin River Delta: a geochemical approach. *Org. Geochem.* **39** (9), 1302–1318.
- Leenheer, J. A. 1981 Comprehensive approach to preparative isolation and fractionation of dissolved organic carbon from natural waters and wastewaters. *Environ. Sci. Technol.* **15** (5), 578–587.
- Leenheer, J. A. & Croué, J.-P. 2003 Characterizing aquatic dissolved organic matter. *Environ. Sci. Technol.* **37** (1), 18A–26A.
- Li, C.-W., Benjamin, M. M. & Korshin, G. V. 2000 Use of UV spectroscopy to characterize the reaction between NOM and free chlorine. *Environ. Sci. Technol.* **34** (12), 2570–2575.
- Li, J., Wen, Y., Zhou, Q., Xingjie, Z., Li, X., Yang, S. & Lin, T. 2008 Influence of vegetation and substrate on the removal and transformation of dissolved organic matter in horizontal subsurface-flow constructed wetlands. *Bioresource Technol.* **99** (11), 4990–4996.
- Li, A., Zhao, X., Mao, R., Liu, H. & Qu, J. 2014 Characterization of dissolved organic matter from surface waters with low to high dissolved organic carbon and the related disinfection byproduct formation potential. *J. Hazard. Mater.* **271**, 228–235.
- Marhaba, T. F. & Van, D. 2000 The variation of mass and disinfection by-product formation potential of dissolved organic matter fractions along a conventional surface water treatment plant. *J. Hazard. Mater.* **74** (3), 133–147.
- McGeehin, M. A., Reif, J. S., Becher, J. C. & Mangione, E. J. 1993 Case-control study of bladder cancer and water disinfection methods in Colorado. *Am. J. Epidemiol.* **138** (7), 492–501.
- Richardson, S. D., Plewa, M. J., Wagner, E. D., Schoeny, R. & Demarini, D. M. 2007 Occurrence, genotoxicity, and carcinogenicity of regulated and emerging disinfection by-products in drinking water: a review and roadmap for research. *Mutat. Res.-Rev. Mutat.* **636** (1–3), 178–242.
- Rook, J. J. 1976 Haloforms in drinking water. *J. Am. Water Works Ass.* **68** (3), 168–172.
- Rostad, C. E., Martin, B. S., Barber, L. B., Leenheer, J. A. & Daniel, S. R. 2000 Effect of a constructed wetland on disinfection byproducts: removal processes and production of precursors. *Environ. Sci. Technol.* **34** (13), 2703–2710.
- Schipper, L. A. & McGill, A. 2008 Nitrogen transformation in a denitrification layer irrigated with dairy factory effluent. *Water Res.* **42** (10–11), 2457–2464.
- Scholz, C., Jones, T. G., West, M., Ehbair, A. M. S., Dunn, C. & Freeman, C. 2016 Constructed wetlands may lower inorganic nutrient inputs but enhance DOC loadings into a drinking water reservoir in North Wales. *Environ. Sci. Pollut. R.* **23** (18), 18192–18199.
- Sun, X., Sun, L., Lu, Y., Zhang, J. & Wang, K. 2014 Influencing factors of disinfection byproducts formation during chloramination of cyclops metabolite solutions. *J. Environ. Sci.* **26** (3), 575–580.
- Uyak, V. & Toroz, I. 2007 Investigation of bromide ion effects on disinfection by-products formation and speciation in an Istanbul water supply. *J. Hazard. Mater.* **149** (2), 445–451.
- Wang, L. & Wang, B. 2000 Pollution of water sources and removal of pollutants by advanced drinking-water treatment in China. *Schriftenr Ver Wasser Boden Lufthyg* **105**, 413–419.
- Wei, Q., Wang, D., Wei, Q., Qiao, C., Shi, B. & Tang, H. 2008 Size and resin fractionations of dissolved organic matter and trihalomethane precursors from four typical source waters in China. *Environ. Monit. Assess.* **141** (1–3), 347–357.
- Wei, L.-L., Zhao, Q.-L., Xue, S., Jia, T., Tang, F. & You, P.-Y. 2009 Behavior and characteristics of DOM during a laboratory-scale horizontal subsurface flow wetland treatment: effect of DOM derived from leaves and roots. *Ecol. Eng.* **35** (10), 1405–1414.
- Weishaar, J. L., Aiken, G. R., Bergamaschi, B. A., Fram, M. S., Fujii, R. & Mopper, K. 2003 Evaluation of specific ultraviolet absorbance as an indicator of the chemical composition and reactivity of dissolved organic carbon. *Environ. Sci. Technol.* **37** (20), 4702–4708.
- Xu, B., Gao, N.-Y., Sun, X.-F., Xia, S.-J., Simonnot, M.-O., Causserand, C., Rui, M. & Wu, H.-H. 2007 Characteristics of organic material in Huangpu River and treatability with the O₃-BAC process. *Sep. Purif. Technol.* **7** (2), 348–355.
- Xu, S., Zhou, S., Xing, L., Shi, P., Shi, W., Zhou, Q., Pan, Y., Song, M.-Y. & Li, A. 2019 Fate of organic micropollutants and their biological effects in a drinking water source treated by a field-scale constructed wetland. *Sci. Total Environ.* **682**, 756–764.
- Yang, Y., Lu, J., Yu, H. & Yang, X. 2016 Characteristics of disinfection by-products precursors removal from micro-polluted water by constructed wetlands. *Ecol. Eng.* **93**, 262–268.
- Zhi-sheng, L., Jun, Y., Li, L. & Yu-juan, Y. 2009 Characterization of NOM and THM formation potential in reservoir source water. *Desalin. Water Treat.* **6** (1–3), 1–4.
- Zhou, S., Zhu, S., Shao, Y. & Gao, N. 2015 Characteristics of C-, N-DBPs formation from algal organic matter: role of molecular weight fractions and impacts of pre-ozonation. *Water Res.* **72**, 381–390.

First received 9 October 2020; accepted in revised form 5 January 2021. Available online 20 January 2021